Supporting Information For

Fuel purification, Lewis acid and aerobic oxidation catalysis performed by a microporous Co-BTT (BTT^{3-} = 1,3,5-benzenetristetrazolate) framework having coordinatively unsaturated sites

Shyam Biswas,[a] Michael Maes,[b] Amarajothi Dhakshinamoorthy,[c] Mark Feyand,[a] Dirk E. De Vos,[b] Hermenegildo Garcia,[c] and Norbert Stock*[a]

[a] *Institut für Anorganische Chemie, Christian-Albrechts-Universität, Max-Eyth-Strasse 2, 24118 Kiel, Germany. E-mail: stock@ac.uni-kiel.de; Tel: +49-4318801675; Fax: +49-4318801775*
[b] *Centre for Surface Chemistry and Catalysis, Katholieke Universiteit Leuven, Kasteelpark Arenberg 23, 3001 Leuven, Belgium*
[c] *Instituto Universitario de Tecnología Química CSIC-UPV and Departamento de Química, Universidad Politécnica de Valencia, Av. De los Naranjos s/n, 46022 Valencia, Spain*

Table of Contents:

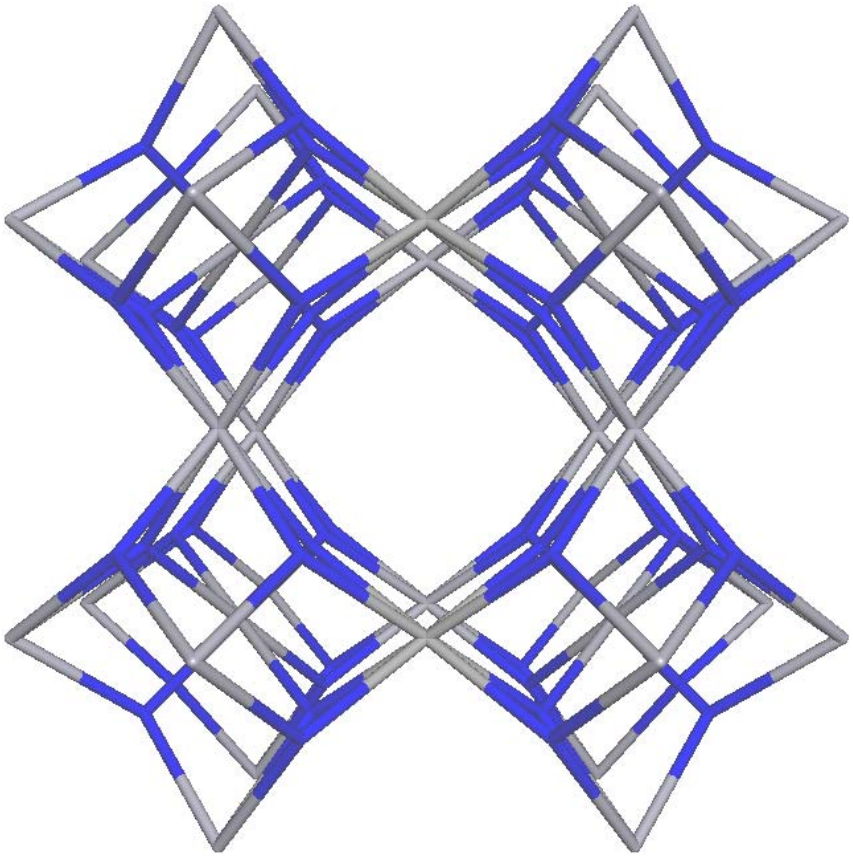

Fig. S1. Wire representation of a portion of the framework of **1** (or **2**) showing its 3D topological connectivity considering BTT ligands and square-planar $[M_4Cl]^{7+}$ units (M = Co, **1**; Cd, **2**) as 3 (blue) and 8 (grey) – connected nodes, respectively, to form the (3,8)-connected "Moravia" net.

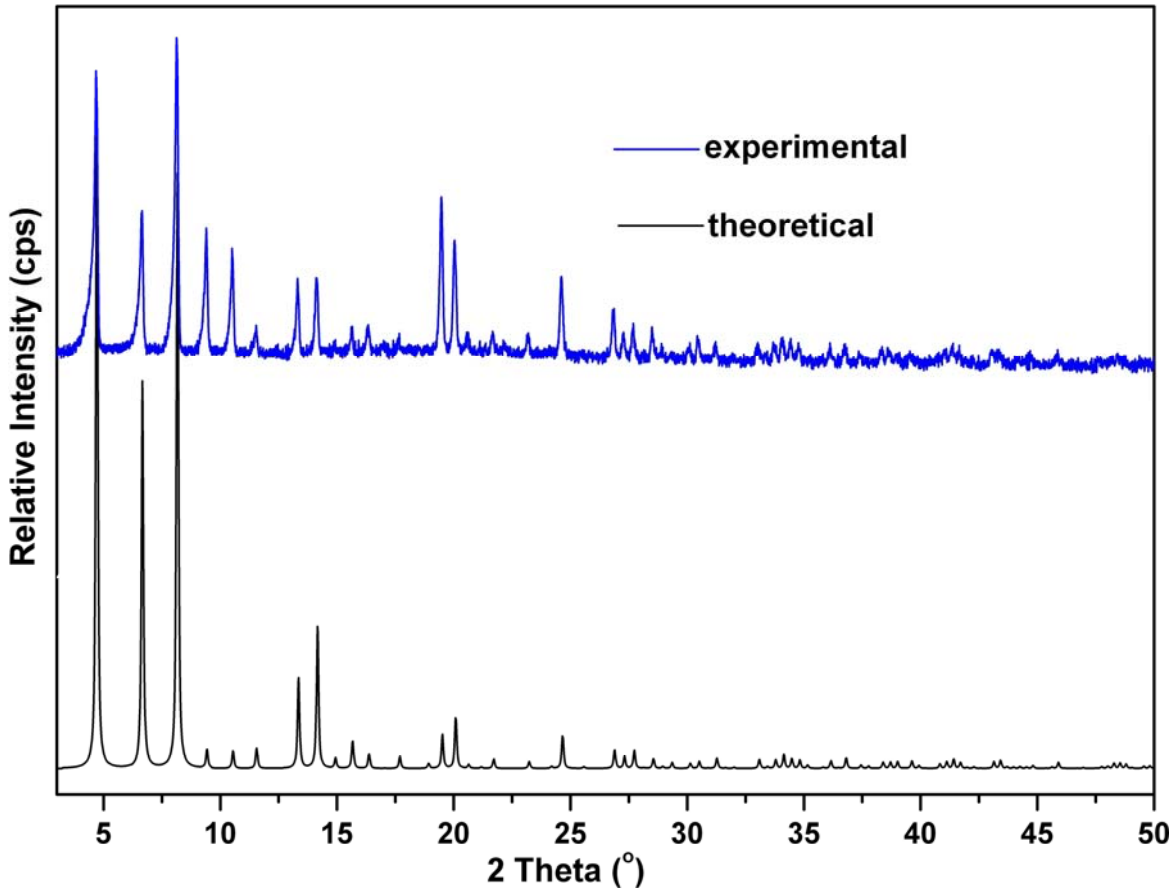

Fig. S2. Theoretical (black) and experimental (blue) XRPD patterns of **1**.

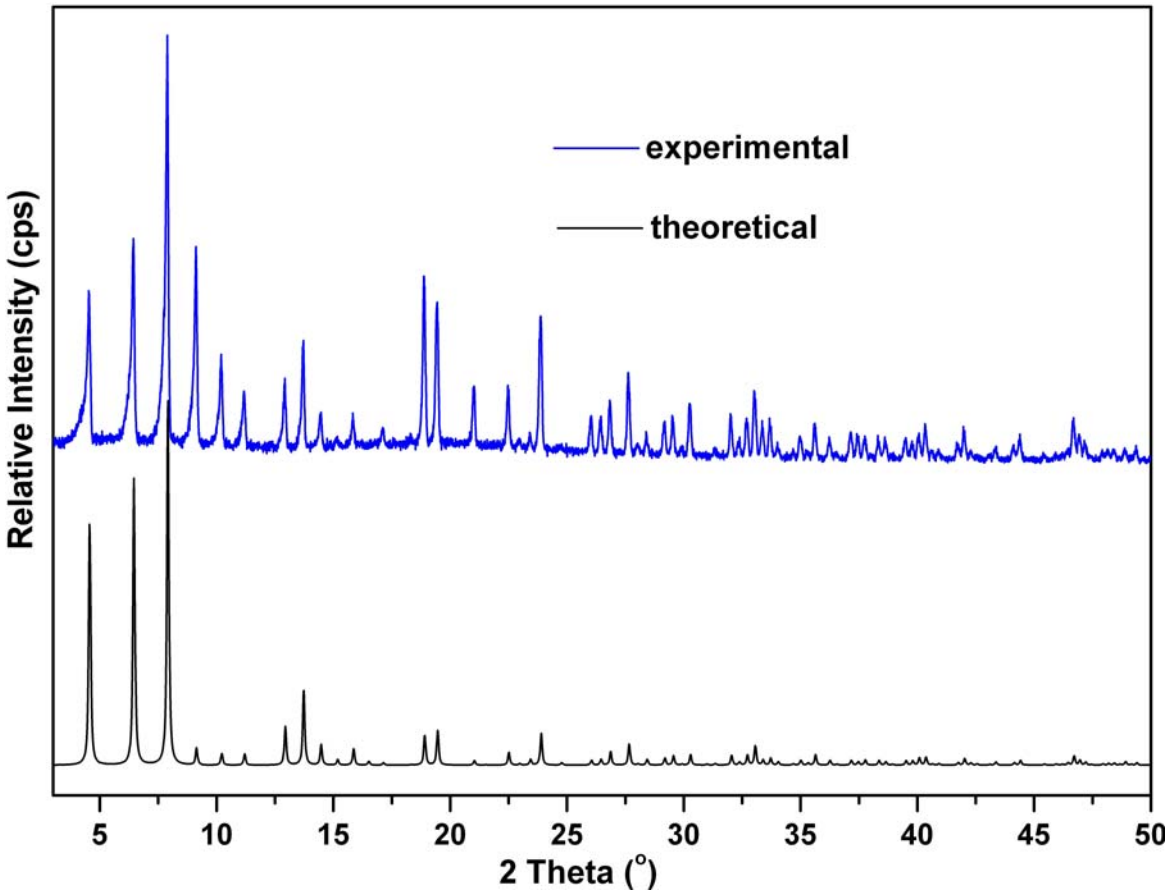

Fig. S3. Theoretical (black) and experimental (blue) XRPD patterns of **2**.

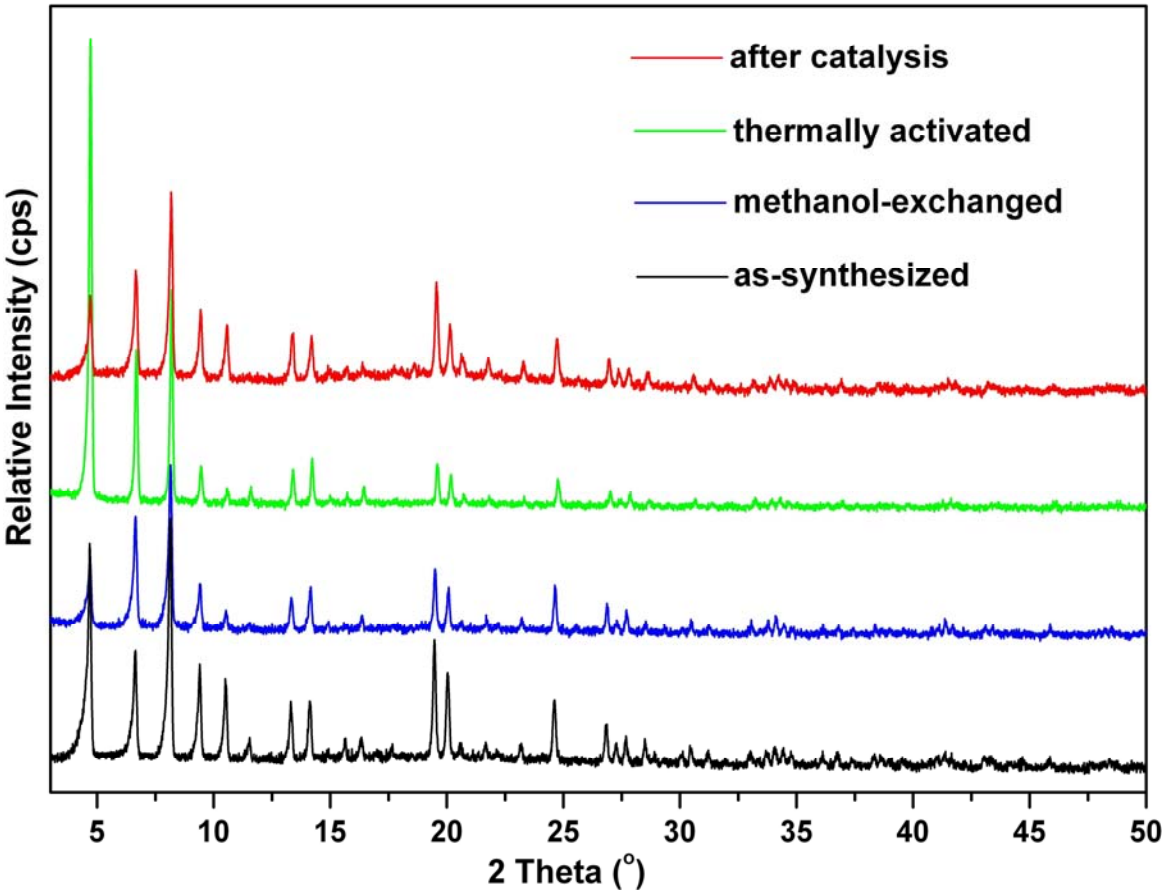

Fig. S4. XRPD patterns of **1** in different forms: as-synthesized (black), methanol-exchanged (blue), thermally activated (green), and after use in ring-opening of styrene oxide with methanol for thrice (red).

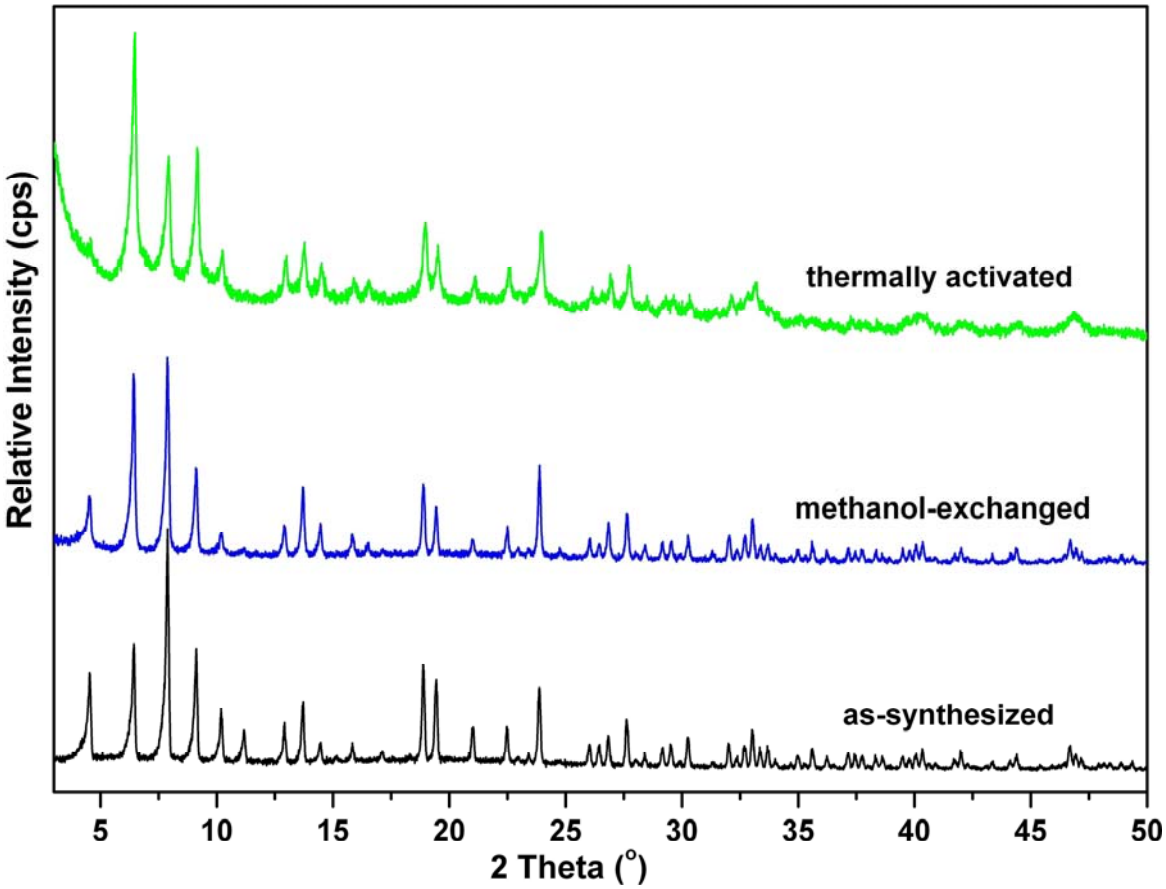

Fig. S5. XRPD patterns of **2** in different forms: as-synthesized (black), methanol-exchanged (blue), and thermally activated (green).

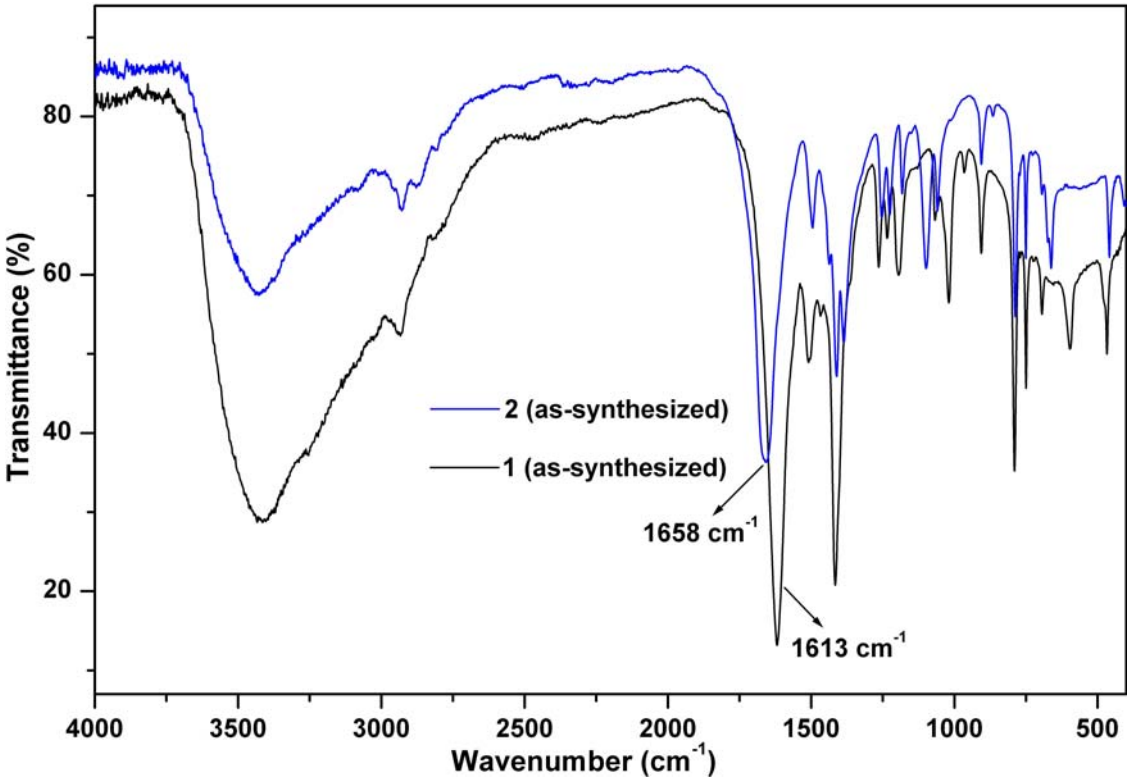

Fig. S6. Comparison between the FT-IR spectra of as-synthesized **1** (black) and **2** (blue).

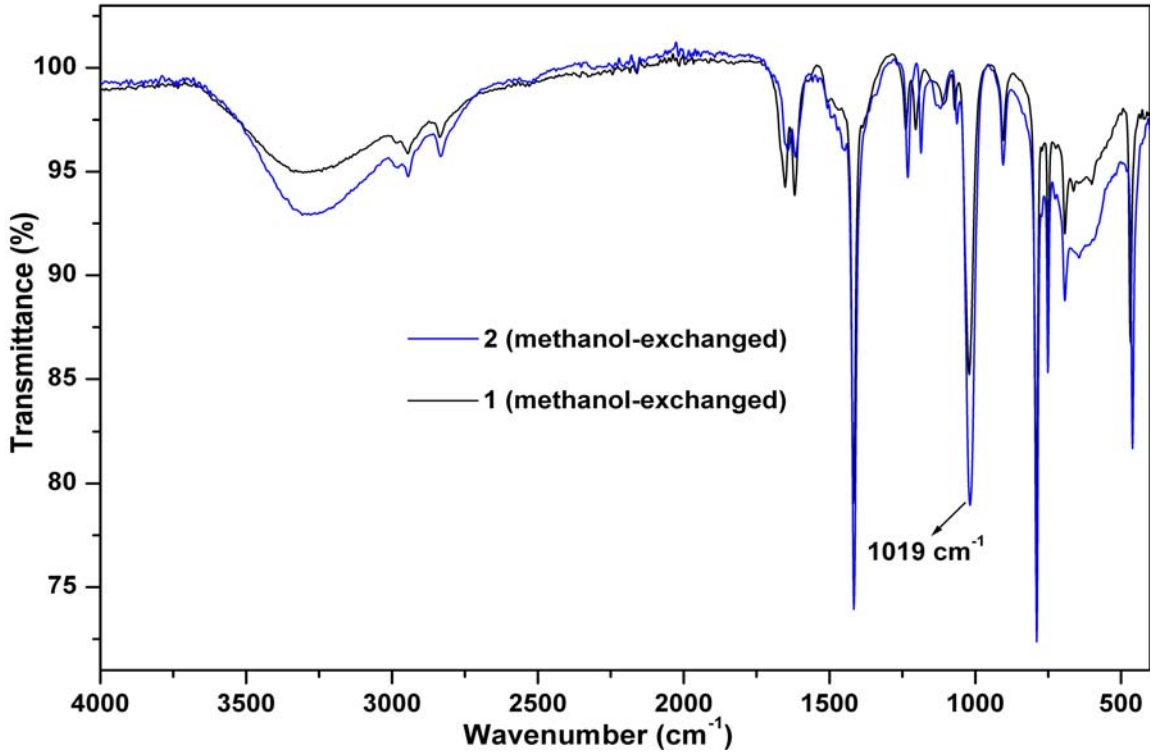

Fig. S7. Comparison between the FT-IR spectra of methanol-exchanged **1** (black) and **2** (blue).

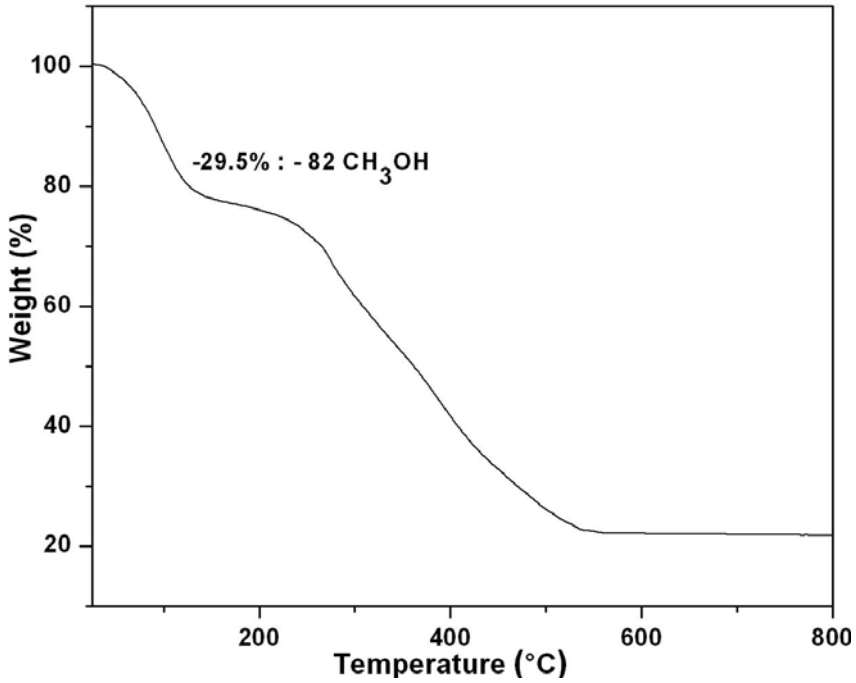

Fig. S8. TG analysis of methanol-exchanged **1**.

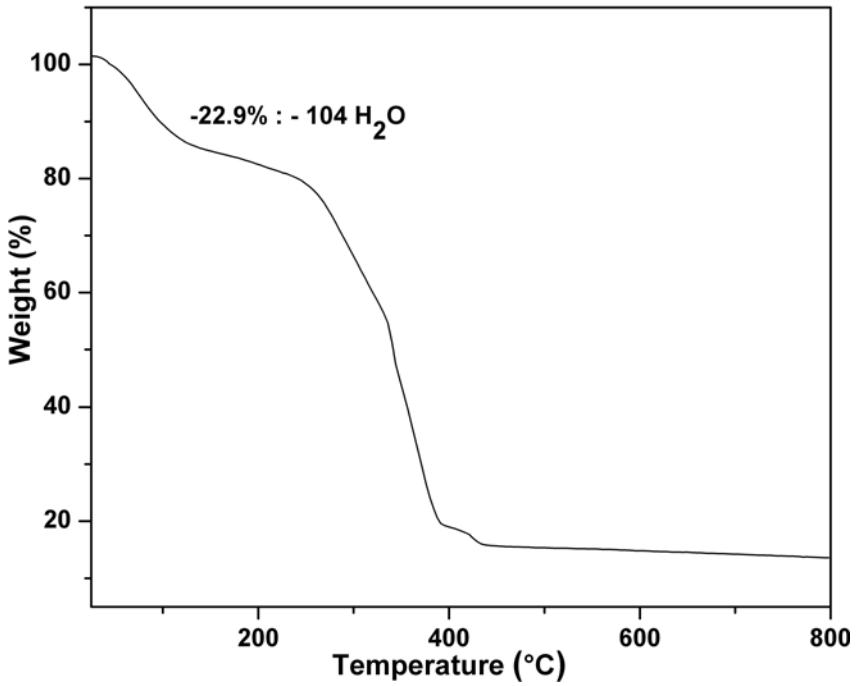

Fig. S9. TG analysis of hydrated **1**.

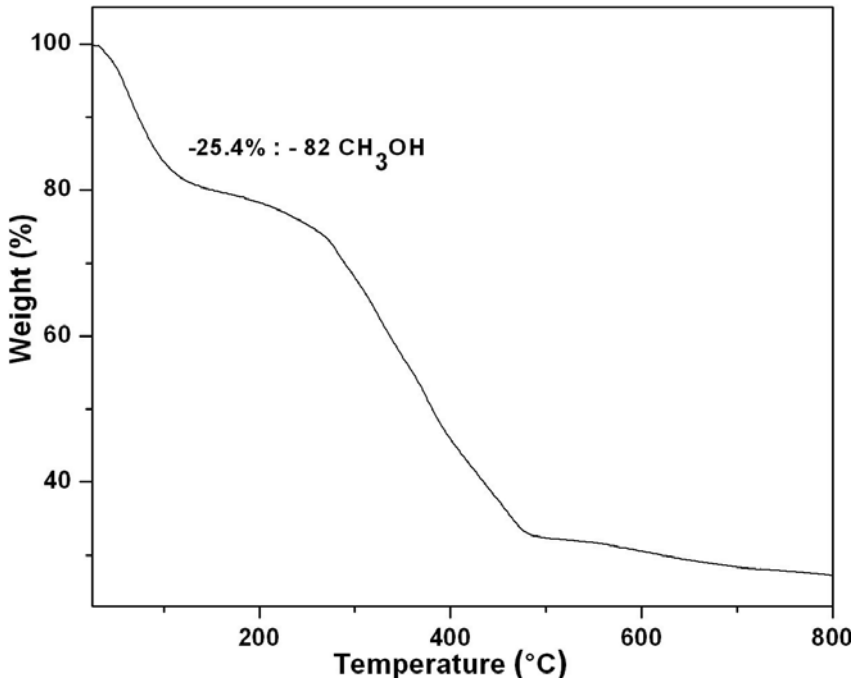

Fig. S10. TG analysis of methanol-exchanged **2**.

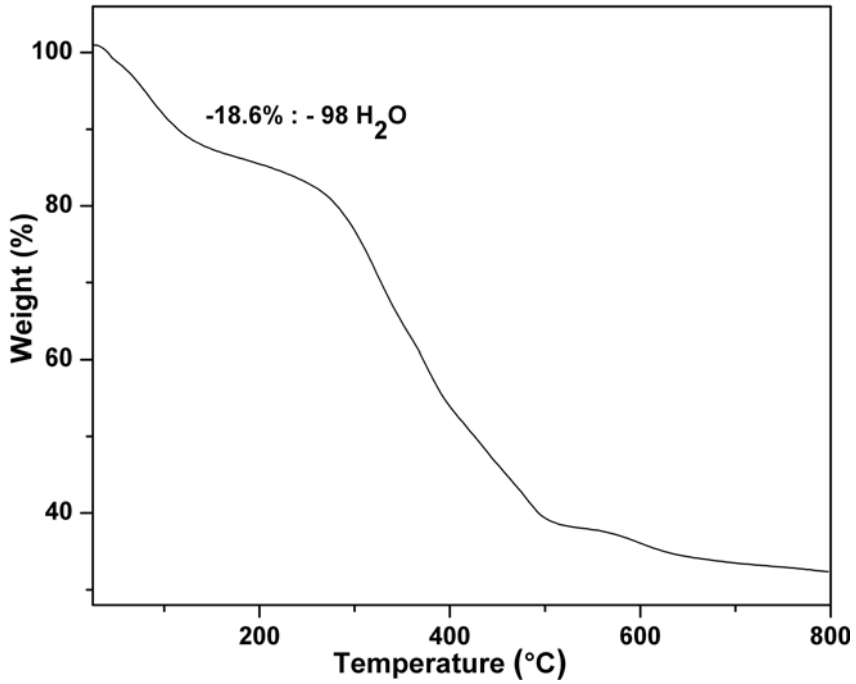

Fig. S11. TG analysis of hydrated **2**.

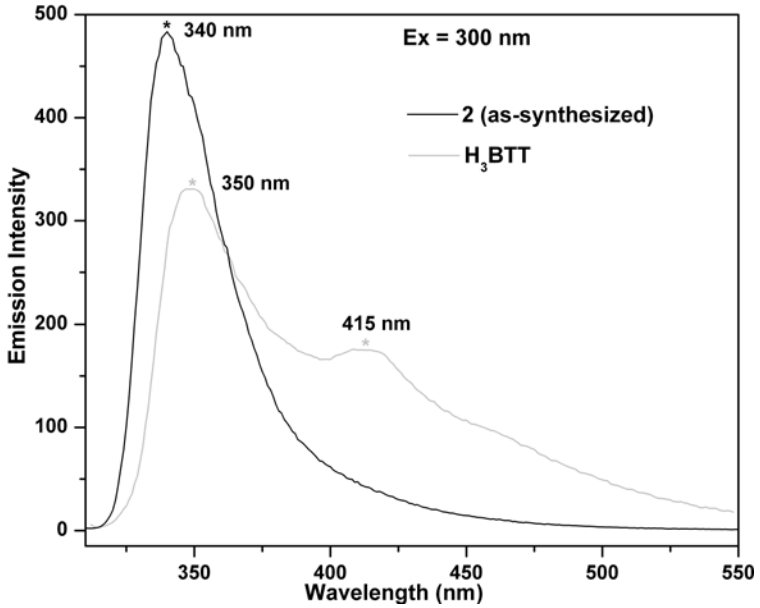

Fig. S12. Solid-state photoluminescence spectra of as-synthesized **2** and free H_3BTT ligand.

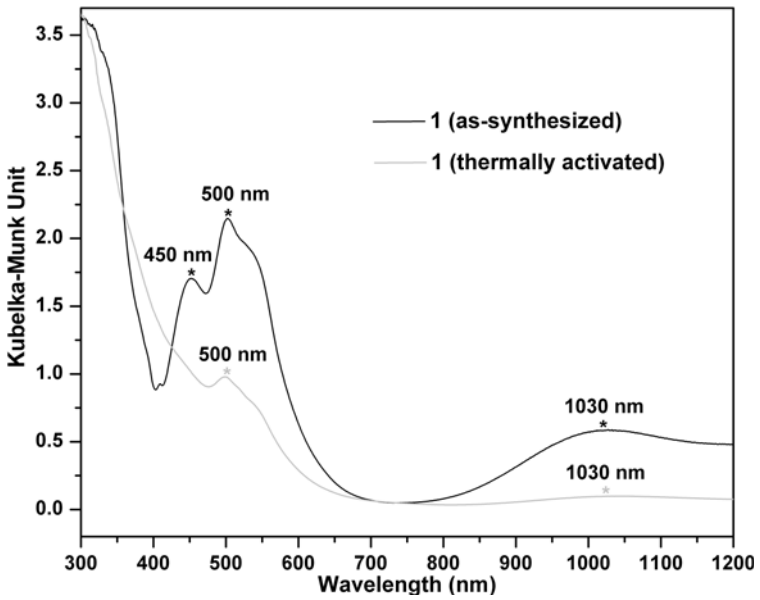

Fig. S13. Solid-state UV-Vis spectra of as-synthesized and thermally activated **1**.

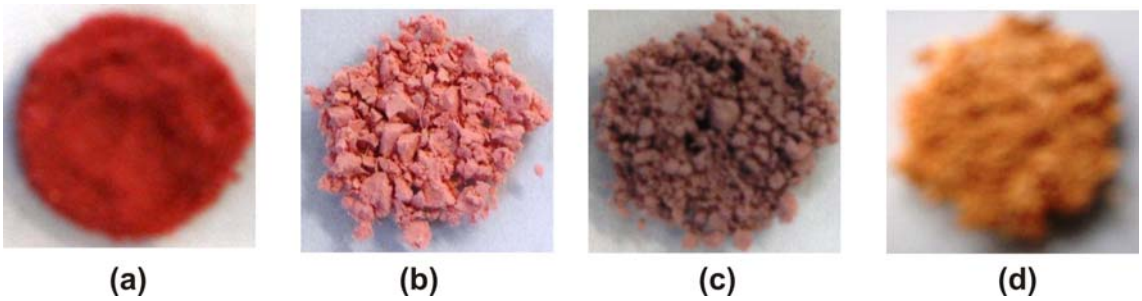

Fig. S14. Photos of **1** showing colour changes in different forms: (a) as-synthesized, (b) methanol-exchanged, (c) thermally activated and (d) after catalysis.

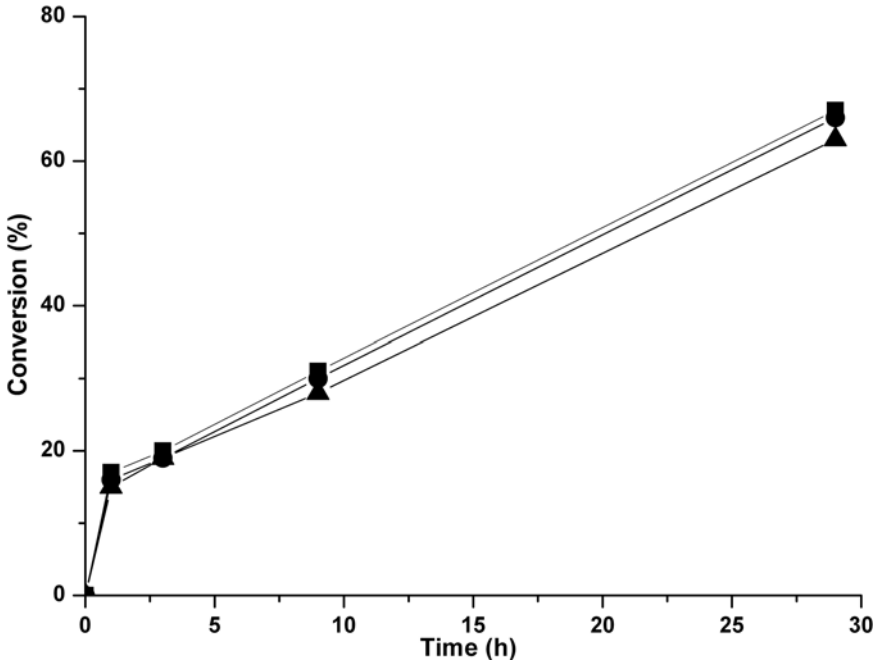

Fig. S15. Reusability test for ring opening of epoxide with methanol using thermally activated **1** as catalyst. Squares, circles and triangles correspond to the first, second and third cycle, respectively. Reaction conditions: (a) styrene oxide (0.1 mL), thermally activated **1** (20 mg), methanol (5 mL), 50 ºC.

Table S1. Elemental analyses of the compounds in different forms.

Compound	Molecular Formula	$C_{obs.}$ / $C_{cal.}$ (%)	$H_{obs.}$ / $H_{cal.}$ (%)	$N_{obs.}$ / $N_{cal.}$ (%)
1-as-synthesized	$[Co(C_4H_9NO)_6]_3[(Co_4Cl)_3(C_9H_3N_{12})_8(H_2O)_{12}]_2 \cdot 12H_2O$	30.34 / 30.56	3.21 / 3.34	34.27 / 34.65
1-methanol-exchanged	$[Co(CH_3OH)_6]_3[(Co_4Cl)_3(C_9H_3N_{12})_8(CH_3OH)_{12}]_2 \cdot 40(CH_3OH)$	30.63 / 30.50	3.97 / 4.25	30.29 / 30.22
1-hydrated	$[Co(H_2O)_6]_3[(Co_4Cl)_3(C_9H_3N_{12})_8(H_2O)_{12}]_2 \cdot 62(H_2O)$	21.53 / 21.23	3.51 / 3.16	32.97 / 33.01
2-as-synthesized	$[Cd(C_3H_7NO)_6]_3[(Cd_4Cl)_3(C_9H_3N_{12})_8(H_2O)_{12}]_2 \cdot 14(H_2O) \cdot 4(C_3H_7NO)$	25.17 / 25.20	2.63 / 2.79	29.64 / 29.95
2-methanol-exchanged	$[Cd(CH_3OH)_6]_3[(Cd_4Cl)_3(C_9H_3N_{12})_8(CH_3OH)_{12}]_2 \cdot 40(CH_3OH)$	25.96 / 26.24	3.43 / 3.66	26.12 / 26.00
2-hydrated	$[Cd(H_2O)_6]_3[(Cd_4Cl)_3(C_9H_3N_{12})_8(H_2O)_{12}]_2 \cdot 56(H_2O)$	18.05 / 18.24	2.73 / 2.59	28.15 / 28.36

Table S2. Bond lengths (Å) for **1**.

Co(1)-O(1)	2.082(7)	N(2)-N(2)#6	1.317(7)
Co(1)-N(2)#1	2.098(3)	N(2)-N(1)	1.337(4)
Co(1)-N(2)	2.098(3)	N(1)-C(1)	1.348(4)
Co(1)-N(2)#2	2.098(3)	C(2)-C(3)#7	1.390(4)
Co(1)-N(2)#3	2.098(3)	C(2)-C(3)	1.390(4)
Co(1)-Cl(1)	2.6007(12)	C(2)-C(1)	1.448(7)
Cl(1)-Co(1)#1	2.6007(12)	C(1)-N(1)#6	1.348(4)
Cl(1)-Co(1)#4	2.6007(12)	C(3)-C(2)#8	1.390(4)
Cl(1)-Co(1)#5	2.6007(12)		

Symmetry operators used to generate equivalent atoms are #1: -x, y, -z+1; #2: -x, y, z; #3: x, y, -z+1; #4: x, z, -y+1; #5: -x, -y+1, -z+1; #6: x, -z+1, -y+1; #7: y, -z+1, -x+1; #8: -z+1, x, -y+1.

Table S3. Bond lengths (Å) for **2**.

Cd(1)-O(1)	2.301(8)	C(1)-N(1)#6	1.335(4)
Cd(1)-N(2)#1	2.329(3)	C(1)-N(1)	1.335(4)
Cd(1)-N(2)#2	2.329(3)	C(1)-C(2)	1.476(7)
Cd(1)-N(2)	2.329(3)	N(1)-N(2)	1.326(4)
Cd(1)-N(2)#3	2.329(3)	N(2)-N(2)#6	1.295(6)
Cd(1)-Cl(1)	2.8032(6)	C(3)-C(2)#7	1.385(4)
Cl(1)-Cd(1)#4	2.8032(6)	C(3)-C(2)	1.385(4)
Cl(1)-Cd(1)#5	2.8032(6)	C(2)-C(3)#8	1.385(4)
Cl(1)-Cd(1)#2	2.8032(6)		

Symmetry operators used to generate equivalent atoms are #1: x, -y, z; #2: -x+1, y, z; #3: -x+1, -y, z; #4: -z+1, -y, x; #5: -x+1, -y, -z+1; #6: -z+1, y, -x+1; #7: y+1, -z, -x+1; #8: -z+1, x-1, -y.